

HYDRODYNAMIC OF A PELTON NOZZLE: CFD COMPARISON BETWEEN STRUCTURED AND UNSTRUCTURED MESH

F. Nascimben, G. Zanetti, G. Cavazzini

Abstract: To properly reproduce the physics of the Pelton jet, one of the key points that must be carefully considered is the computational grid, whose selection and design determines the accuracy of the results and computational costs. In this paper, a comparison between structured and unstructured mesh approaches for the simulation of a Pelton nozzle flow is reported, analysing the influence that the mesh design process can have on jet quality and computational costs. The results confirmed the structured mesh approach to be the best option for Pelton injectors simulations.

Keywords: Pelton nozzle, structured, unstructured, jet quality

1 Introduction

The numerical simulation of the hydrodynamic behaviour of Pelton nozzles (and Pelton turbines in general) has always been pretty challenging due to the complex interaction occurring between water and air at the nozzle exit, which usually requires particular attention both from the numerical method choice and the meshing strategy.

As reported by Jiyuan et al. [1], two possible theoretical approaches for constructing the numerical grid are available and they are known as structured and unstructured meshing approaches.

The first one regards all those numerical grids consisting of cells with regularly shaped elements with four-nodal corner points in 2D problems cases and hexahedron-shaped elements and eight-nodal corner for three-dimensional cases. On the other hand, the unstructured meshing approach relies on non-regularly shaped elements, e.g. triangles for planar geometries and tetrahedrons or (in recent times) polyhedrons for 3-D geometries. The structured mesh usually guarantees the best results, but it requires heavy pre-processing operations and it's difficult to be applied to complex geometries, which are the typical field of application for unstructured meshes.

Regarding the applications of such meshing strategies to Pelton injectors, literature provides many different examples, which substantially differ one from each other for the type of element used in the grid construction.

A completely structured mesh has been used by Semlitsch to analyze both the effect of the disturbances developing inside the distributor line of a 6-nozzles Pelton turbine [2] and the quality of the jet exiting from the nozzles [3] at part-load conditions. Another example of structured mesh applied to Pelton injectors has been reported by Bajracharya et al. [4] to study the nozzle erosion caused by sediments.

Concerning the unstructured mesh approach, both Stivala et al. [5] and Chongji et al. [6] conducted their numerical investigation on Pelton jet profiles relying on tetrahedral meshes. Other examples of unstructured meshing techniques applied to Pelton injectors numerical analyses have been reported in literature by Messa et al. [7] and Decaix et al. [8], who conducted their analyses relying on cartesian meshes, i.e. numerical grids whose elements are all cubes aligned to the Cartesian coordinate frame of the domain. More recently, CFD software has begun to give users the possibility to also use polyhedra as elements for numerical grid construction. This feature was exploited by both Fan et al. [9] and Liu et al. [10] in their studies concerning Pelton turbine flow instabilities and erosion inside a large Pelton nozzle, respectively.

All these studies on the hydrodynamic behaviour of Pelton nozzles demonstrate that both structured and unstructured meshing approaches lead to valuable results, but it is not simple to scientifically determine which one is more convenient in terms of accuracy and computational costs when the focus falls on Pelton injectors flow.

Therefore, the present work tries to fill this lack of knowledge, comparing how grids deriving from structured and unstructured meshing techniques perform under the same flow conditions.

In Section 2, the numerical set-up is reported, describing the simulations operating conditions (in terms of nozzle opening and flow rates) and the meshing strategy followed for the construction of both the structured and unstructured grids. Inside Section 3, the results are briefly analysed and the comparison between the structured and unstructured grid performance is carried out. Finally, Section 4 resumes the results coming from the analysis and presents the conclusions deriving from the present study.

2 Numerical Set - Up

The flow inside the Pelton injector installed inside the Hydropower Laboratory of the University of Padova (whose geometry is characterised by a nozzle diameter equal to 36 mm and a needle tip semi-angle of 25° as reported inside Fig. 1) has been simulated considering two different opening conditions (50% and 100% opening, expressed as the ratio between the needle stroke s and the nozzle diameter d) and 4 different flow rate conditions for each opening case, leading to the 8 total different combinations reported inside Tab. 1.

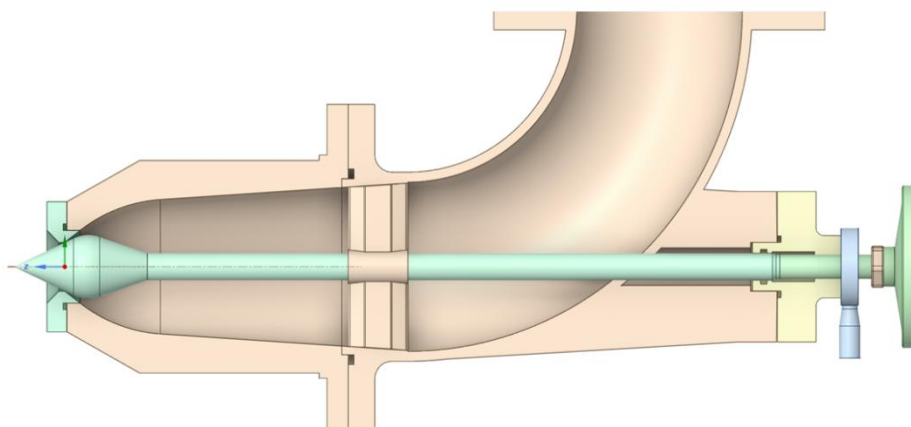


Fig. 1. Some details of the nozzle geometry involved in the case study. The nozzle diameter is equal to 36 mm, while the needle tip semi-angle is 25° .

As reported inside Fig. 1, the geometry of the entire nozzle is pretty complex, since also the fins and the curve have been considered, together with the inlet pipe, whose length has been chosen equal to 1.25 m (which is equal to 10 times the pipe diameter $d_{PIPE} = 125$ mm) in order to have fully developed flow conditions at the curve entrance. A cylinder of 360 mm diameter and 360 mm long (both equal to 10 times the nozzle diameter) has been inserted after the nozzle outlet with the aim of setting the pressure boundary conditions at a certain distance from the injector outlet and reducing to the minimum the influence that such boundary conditions can exert on it.

For each opening condition, 3 structured meshes configurations (coarse, medium, fine) and 3 unstructured meshes configurations (coarse, medium, fine) have been created following these two guidelines:

- The ratio between the number of elements of two consecutive meshes configurations should be nearly equal to 2 – this allows to apply the criterion proposed by Celik et al. [11] for studying results convergence.
- The number of nodes of structured and unstructured grids should be nearly the same for the same opening and flow rate conditions and mesh configurations – this allows to perform the comparison between structured and unstructured grids results, since CFX (which is the CFD software used for running all the simulations) is a node-based solver.

In all the structured configurations, the curve mesh has been generated following a non-structured approach, setting a certain number of prism layers at the curve wall and filling the curve domain with tetrahedrons. This choice is due to the presence of the needle stick, which made the curve geometry really complex and impossible to mesh following a fully structured approach. In the unstructured case, fluid domain has been meshed only relying on tetrahedrons and setting prism layers at the domain walls, with subsequent refinements close to the nozzle outlet.

Inside Tab. 1 the information about nodes and elements number are reported for all the mesh configurations, while some details of both structured and unstructured mesh are shown inside Fig. 2 for the 50% opening condition.

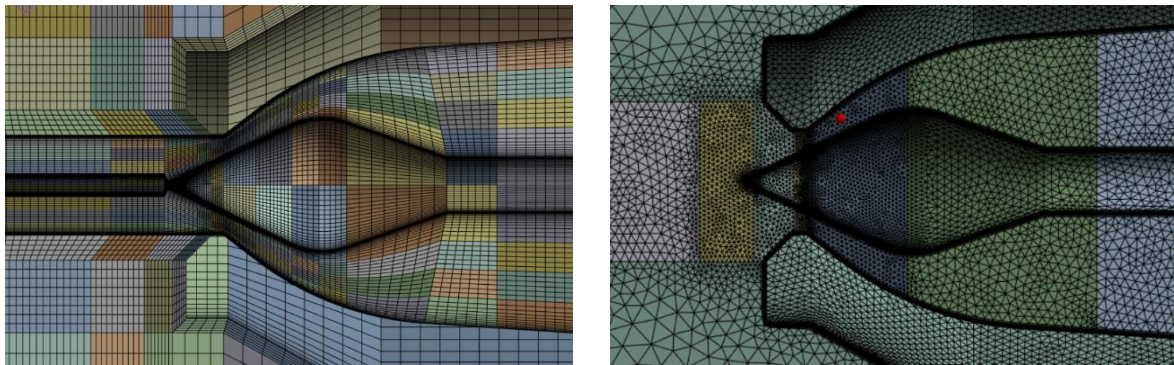
All the configurations have been solved using CFX as CFD solver, considering steady state simulations. The interaction between the two phases (air and water) has been reproduced through the use of a *non-homogeneous model* due to the complexity of the flow developing after the pipe curve and the fins.

A *standard free surface model* has been selected for correctly reproducing the water-air interface at the jet external surface, setting the water-air surface tension equal to 0.072 N·m and the drag coefficient between the phases equal to 0.44. The *k- ω SST* turbulence model has been considered to close the turbulence problems, together with the hypothesis of isothermal flow, which has given the possibility to neglect the energy equation. A residual target of 10^{-4} for the RMS residuals has been set as convergence condition for all the monitors. Gravity effect has also been taken into account, setting the gravitational acceleration equal to 9.81 m/s² on the y-axis negative direction.

Both air and water have been modelled as continuous fluid, setting their density respectively equal to $\rho_{AIR} = 1.185$ kg/m³ and $\rho_{WATER} = 997$ kg/m³ and their dynamic viscosity respectively equal to $\mu_{AIR} = 1.83 \cdot 10^{-5}$ Pa·s and $\mu_{WATER} = 8.90 \cdot 10^{-4}$ kg/m³ Pa·s.

OPENING	MESH	STRUCTURED		UNSTRUCTURED		FLOW RATE	INLET VELOCITY
		NNODES	NELEMENTS	NNODES	NELEMENTS	Q _v	V _{IN}
		[-]	[-]	[-]	[-]	[L/s]	[m/s]
0.5	COARSE	0.662M	0.750M	0.664M	2.540M	12.1	0.986
	MEDIUM	1.344M	1.501M	1.363M	5.578M	14.8	1.207
	FINE	2.572M	3.011M	2.575M	10.615M	17.1	1.394
1	COARSE	0.823M	0.869M	0.827M	2.971M	19.1	1.559
	MEDIUM	1.562M	1.744M	1.540M	5.665M	14.1	1.150
	FINE	3.038M	3.503M	3.062M	11.557M	17.3	1.409
						20.0	1.627
						22.3	1.819

Table 1: Information concerning meshes configurations and inlet boundary conditions



(a) Pelton nozzle structured mesh

(b) Pelton nozzle unstructured mesh

Fig. 2. Some details concerning the structured (a) and unstructured (b) mesh

Concerning boundary conditions, a *Velocity Inlet* condition has been specified at the *Inlet* section of the fluid domain together with the value of the inlet velocity (which has been determined dividing the flow rate by the area of the inlet pipe section), while the inlet water volume fraction has been set equal to 1.

In addition, the external surfaces of the outlet cylinder have been defined as *Opening* boundary conditions, setting a relative pressure equal to 0 Pa, together with a Zero Gradient condition for both turbulence and volume fractions.

All the remaining surfaces have been addressed as stationary *walls*, setting the *no slip* condition on such boundaries. Every coarse simulation has been initialised filling the fluid domain from inlet section to the needle nose cone start with water flowing at inlet conditions to speed up all the simulation process, while simulations with medium and fine meshes have been initialised with the final results obtained from the corresponding coarse mesh.

3 Results

3.1 Grid convergence study

Before proceeding to the results analysis, a grid convergence study has been conducted to understand the convergence level guaranteed by the two meshing strategies.

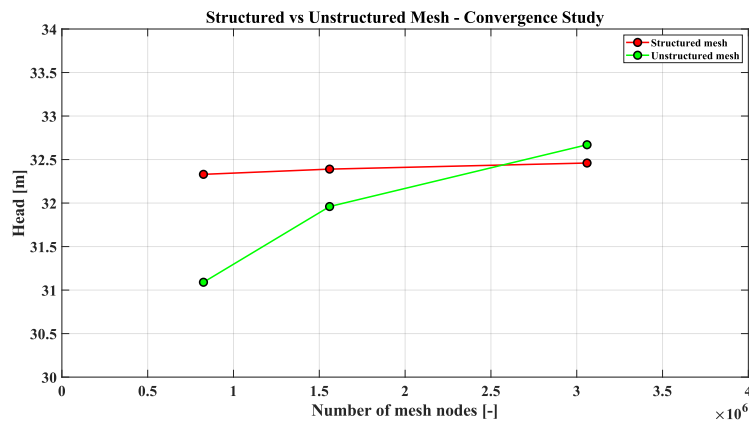


Fig. 3. Grid convergence trends using structured and unstructured mesh for the case of 50% opening and 20 m³/s flow rate.

As previously mentioned, the grid convergence study has been carried on following the procedure proposed by Celik et al. [11] and taking the head measured at the domain inlet as convergence evaluation parameter. The typical convergence trend obtained by structured and unstructured cases for the same boundary conditions is visually reported inside Fig. 3.

As can be observed, the structured mesh reports a nearly flat convergence trend, which is the sign of convergence achievement, while the unstructured mesh one still presents an increasing behaviour, probably showing the need of another further meshing refinement step to reach convergence.

This fact has also been confirmed by the grid convergence study whose data are reported inside Tab. 2. Inside this table, performances in terms of CPU time for every single simulation and total CPU time to complete an entire meshing cycle have been reported too. As it can be observed, structured meshes seems to behave better in all the cases, reaching solid convergence with a lower CPU time for all the mesh configurations and opening (structured meshes total CPU time was at least half of the unstructured mesh CPU time for all the configurations). Unstructured meshing approach really struggles to reach convergence, in particular considering the 50% opening case, where coarse and medium mesh needed way more CPU seconds to complete a full grid convergence study cycle for the same conditions without finally reaching a solid convergence status.

This aspect highlights, for an unstructured mesh approach, the need of way more nodes and elements to reach the same convergence level that can be obtained relying on structured meshes. An interesting feature that must be underlined is the fact that the extrapolated results for the unstructured mesh are in fair agreement with the ones coming from the structured meshing analysis, highlighting the fact that both approaches nearly lead to the same results.

3.2 Analysis of the results

After having studied the grid influence on the final solution for the two meshing approaches, the Authors proceeded to the real results analysis. All the reported contour plots derive from the fine meshes configurations. As can be observed inside Fig. 4, the air-water interface for the 50% opening condition results to be smoother for the structured mesh configurations.

s/D	Q _v	MESH	h [m]	r	p	h _{EXT}	GCI	CPU TIME	TOTAL CPU TIME
[-]	[L/s]	[-]	[m]	[-]	[-]	[m]	[%]	[CPU s]	[CPU s]
0.5 – STR	12.1	COARSE	19,36	1,26	2,83	20,87	-	26730	156600
		MEDIUM	20,09				5,08	23270	
		FINE	20,46				2,54	106600	
	14.8	COARSE	28,98	1,26	2,93	31,20	-	24230	136440
		MEDIUM	30,08				2,67	21730	
		FINE	30,63				1,30	90480	
	17.1	COARSE	38,64	1,26	2,98	41,56	-	23330	121830
		MEDIUM	40,10				2,60	20930	
		FINE	40,83				1,25	77570	
	19.1	COARSE	48,32	1,26	3,01	51,93	-	22100	136340
		MEDIUM	50,13				2,55	20360	
		FINE	51,03				1,22	93880	
0.5 – UNSTR	12.1	COARSE	19,36	1,26	2,54	21,01	-	83810	992210
		MEDIUM	20,13				5,98	122300	
		FINE	20,53				2,95	786100	
	14.8	COARSE	29,01	1,26	2,73	31,36	-	32720	906720
		MEDIUM	30,17				2,94	505800	
		FINE	30,74				1,54	368200	
	17.1	COARSE	38,65	1,26	2,65	41,86	-	28790	576390
		MEDIUM	40,20				3,07	310100	
		FINE	40,98				1,62	237500	
	19.1	COARSE	48,29	1,26	1,87	53,19	-	43110	274610
		MEDIUM	50,10				4,51	151800	
		FINE	51,21				2,86	79700	
1.0 – STR	14.1	COARSE	16,18	1,26	5,79	16,25	-	35870	236740
		MEDIUM	16,19				0,03	64870	
		FINE	16,23				0,12	136000	
	17.3	COARSE	24,25	1,26	0,82	24,62	-	50830	220450
		MEDIUM	24,30				1,34	54820	
		FINE	24,35				1,25	114800	
	20.0	COARSE	32,33	1,26	0,90	32,76	-	49110	195960
		MEDIUM	32,39				1,14	48710	
		FINE	32,46				1,07	98140	
	22.3	COARSE	40,41	1,26	0,82	40,96	-	46170	178600
		MEDIUM	40,48				1,24	42880	
		FINE	40,56				1,15	89550	
1.0 – UNSTR	14.1	COARSE	15,53	1,26	1,04	17,70	-	45360	536240
		MEDIUM	15,98				13,68	96680	
		FINE	16,34				10,64	394200	
	17.3	COARSE	23,31	1,26	1,07	26,43	-	159400	518100
		MEDIUM	23,98				6,72	107500	
		FINE	24,51				5,32	251200	
	20.0	COARSE	31,09	1,26	0,97	35,57	-	55520	346840
		MEDIUM	31,96				7,37	72520	
		FINE	32,67				5,98	218800	
	22.3	COARSE	38,83	1,26	1,17	43,68	-	50130	354630
		MEDIUM	39,95				6,12	100900	
		FINE	40,82				4,74	203600	

Table 2. Mesh convergence study data and mesh performance data

On the other side, for the same number of nodes and a wider number of elements, the air-water jet interface obtained from unstructured mesh configurations results to be really blurred, bringing to the computation of broader jet diameter.

This aspect is surely related to the fact that the structured mesh approach gives the possibility to place a higher number of cells nearby that area, increasing the chances of correctly catching the volume fraction gradients at the jet surface.

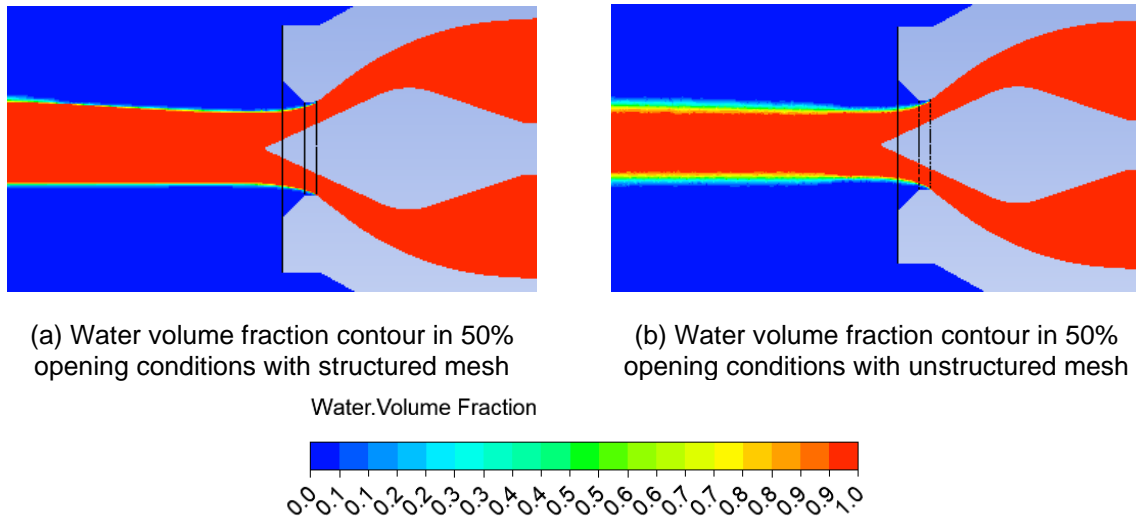
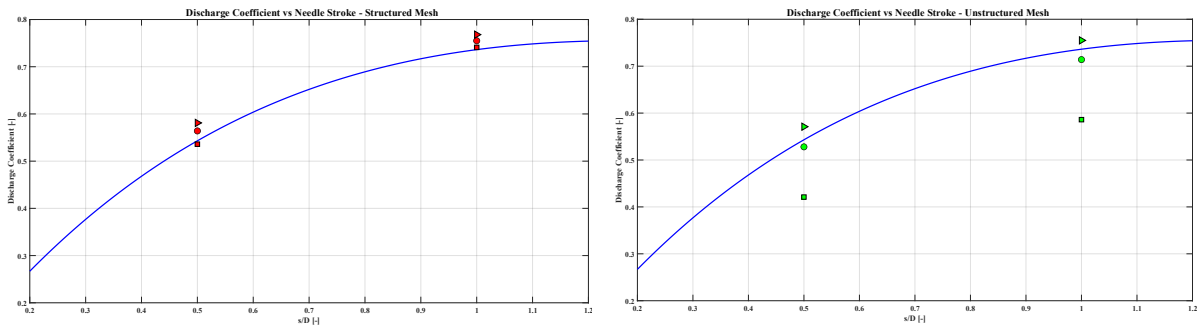


Figure 4. Comparison between structured and unstructured mesh water volume fraction contour for 50% opening conditions

The latter statement is supported by the analysis conducted on the influence of the maximum value of water volume fraction limit considered for the computation of jet diameter and jet velocity for the subsequent definition of the discharge coefficient. As reported inside Fig. 5a – b, correct discharge coefficient values (according to Zhang [12]) are obtained using a structured mesh approach for water volume fraction limit close to 1, while for lower water volume fraction limit the discharge coefficient results to be overestimated. Unstructured mesh approach, on the other hand, requires lower water volume fraction limits to correctly reproduce the effective discharge coefficient value.



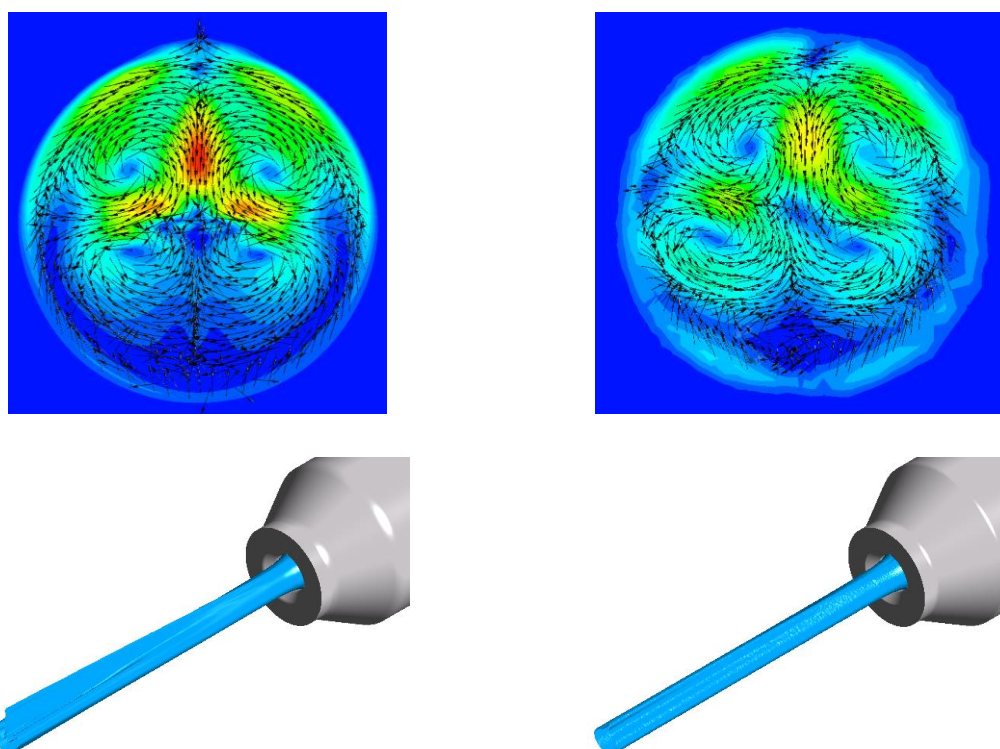
(a) Discharge coefficient computed considering different water volume fraction values using structured fine mesh configurations

(b) Discharge coefficient computed considering different water volume fraction values using unstructured fine mesh configurations

- ▶ 60% water volume fraction limit
- 80% water volume fraction limit
- 99% water volume fraction limit

- ▶ 60% water volume fraction limit
- 80% water volume fraction limit
- 99% water volume fraction limit

Figure 5. Discharge coefficient for different maximum water volume fraction values



(a) Secondary flows developing in 50% opening conditions using a structured mesh approach

(b) Secondary flows developing in 50% opening conditions using a unstructured mesh approach

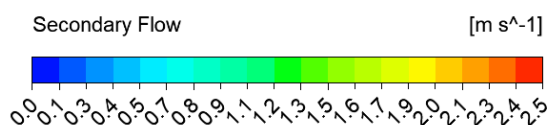


Figure 6. Comparison between structured and unstructured mesh secondary flow contours and jet isosurface for 50% opening conditions

This behavior, once again, is due to the fact that unstructured mesh is not so effective in catching the water-air interface, underestimating the jet diameter for high water volume fraction limits, consequently underestimating the discharge coefficient.

Another aspect that has been qualitatively investigated is the influence that the meshing approach choice can have on the Pelton jet quality. In particular, the secondary flow velocities and velocity vector projection at a distance of 36 mm from the nozzle outlet have been computed following Semlitsch [2]-[3] procedure and compared inside Fig. 6, which also reports, for the 50% opening case, the isosurface of all the points having water volume fraction larger than 0.6.

As it can be observed by looking at Fig. 6, structured meshing approach was able to correctly reproduce the secondary flows developing inside the jet due to the presence of the curve before the Pelton nozzle. On the other hand, unstructured mesh is also able to catch some sort of secondary flows, but they are characterized by a lower intensity and they have no symmetrical behavior. This last fact brings the jet isosurface of unstructured meshing to look more cylindrical than the structured mesh isosurface, not recreating the typical ripple that usually generates on the jet surface on the plane of the pipe curve when a Pelton nozzle is preceded by a pipe bend.

This aspect can be possibly reconducted to diffusion phenomena characterizing unstructured meshes behavior which lead to reduction of turbulence and secondary flows due to poor refinement. This fact further confirms the need of a really large number of mesh nodes and elements when using an unstructured meshing approach, inevitably increasing the computational costs to obtain good results.

Probably, the use of polyhedral elements instead of tetrahedral elements would help in reaching good results with a lower elements number, even though still using an unstructured meshing approach.

4 Conclusions

The present work focused on the analysis of the influence of the meshing approach (structured hexahedral mesh vs. unstructured tetrahedral mesh) for the numerical simulation of the hydrodynamic behaviour of a Pelton nozzle.

Two opening conditions (50% and 100% opening) have been considered, together with 4 different flow rate conditions per each opening case. Structured and unstructured meshes have been generated in three different configurations (coarse, medium, fine) sharing the same number of nodes for the corresponding mesh configuration.

The analysis of the results highlighted the following aspects:

- For the same number of nodes, structured meshes reach convergence in lower CPU time (at least half of the unstructured mesh total CPU time) and give better results in terms of accuracy and agreement with literature data.
- The unstructured mesh configurations are not so effective in catching the sharp interface between air and water on the Pelton jet surface, bringing to jets characterised by broader diameters.
- This last aspect underlines the fact that analysis conducted relying on unstructured meshing approach needs way more nodes, elements and computational costs to reach the same quality results of those analysis conducted using a structured meshing approach.
- The structured meshing approach gave the possibility to correctly catch the secondary flows also for very low opening conditions. Also unstructured meshes are able to catch them, but at a lower intensity.

Finally, structured mesh confirmed to be the best choice, especially for Pelton nozzle jet analysis, when accurate results are needed, and computational resources are not that large. Unstructured meshing approach can be a valuable choice when it is not possible to rely on large pre-processing time but need large computational resources.

Modern polyhedral meshes can help in reducing the elements and nodes number while increasing unstructured mesh results quality and reducing computational time. Future analysis should be carried out to perform a comparison between polyhedral unstructured mesh and hexahedral structured mesh performances.

References

- [1] T. Jiyuan, Y. Guan-Heng, L. Chaoqun, *Chapter 4 - CFD Techniques—The Basics, Computational Fluid Dynamics (Second Edition)*, Butterworth-Heinemann, 2013, Pages 123-175, ISBN 9780080982434, <https://doi.org/10.1016/B978-0-08-098243-4.00004-4>.
- [2] B. Semlitsch. On the Water Jet Quality at Part-Load Operation of Pelton turbines. *Journal of Physics: Conference Series*. 2752. (2024) 012164.
- [3] B. Semlitsch, Effect of inflow disturbances in Pelton turbine distributor lines on the water jet quality, *International Journal of Multiphase Flow*, Volume 174, 2024, 104786, ISSN 0301-9322, <https://doi.org/10.1016/j.ijmultiphaseflow.2024.104786>.
- [4] Bajracharya, Tri Ratna, Shrestha, Rajendra, Sapkota, Anil, Timilsina, Ashesh Babu, Modelling of Hydroabrasive Erosion in Pelton Turbine Injector, *International Journal of Rotating Machinery*, 2022, 9772362, 15 pages, 2022. <https://doi.org/10.1155/2022/9772362>
- [5] D. Stivala et al 2021 IOP Conf. Ser.: Earth Environ. Sci. 774 012106
- [6] Chongji, Zeng & Xiao, Y.X. & Wei, Xu & Tao, Wu & Jin, Zhang & Zhengwei, Wang & Luo, Yongyao. (2016). Numerical Analysis of Pelton Nozzle Jet Flow Behavior Considering Elbow Pipe. *IOP Conference Series: Earth and Environmental Science*. 49. 022005. 10.1088/1755-1315/49/2/022005.
- [7] Messa, Gianandrea & Mandelli, Simone & Malavasi, Stefano. (2018). Hydroabrasive erosion in Pelton turbine injectors: A numerical study. *Renewable Energy*. 130. 474-488. 10.1016/j.renene.2018.06.064.
- [8] Decaix, J.; Münch-Alligné, C. Geometry, Mesh and Numerical Scheme Influencing the Simulation of a Pelton Jet with the OpenFOAM Toolbox. *Energies* 2022, 15, 7451. <https://doi.org/10.3390/en15197451>
- [9] Fan, Wenrui & Sun, Longgang & Guo, Pengcheng. (2024). Investigation on unstable flow characteristics and energy dissipation in Pelton turbine. *Engineering Applications of Computational Fluid Mechanics*. 18. 10.1080/19942060.2024.2304643.
- [10] Liu, J.; Pang, J.; Liu, X.; Huang, Y.; Deng, H. Analysis of Sediment and Water Flow and Erosion Characteristics of Large Pelton Turbine Injector. *Processes* 2023, 11, 1011. <https://doi.org/10.3390/pr11041011>
- [11] I. Celik, U. Ghia, P.J. Roache, Freitas, Chris & Coloman, H & Raad, Peter. (2008). Procedure of Estimation and Reporting of Uncertainty Due to Discretization in CFD Applications. *J. Fluids Eng.* 130. 078001. 10.1115/1.2960953.
- [12] Z. Zhang. *Pelton Turbines*. (2016) 10.1007/978-3-319-31909-4.

Author(s)

Eng. Francesco NASCIMBEN,
Università degli Studi di Padova
Department of Industrial Engineering
Turbomachinery & Energy Systems Research Group (TES)
Via Venezia 1, Padova, 35131, Italy
E-mail: francesco.nascimben@phd.unipd.it

Francesco Nascimben graduated in 2020 in Mechanical Engineering at the University of Padova with a Master thesis in collaboration with prof. Jens Walther of the DTU.

After one year of work as a Research Grant fellow for the Department of Industrial Engineering of the University of Padua, he is currently working as a PhD student for the same department. His research focuses on multi-phase flows, in particular sediments transport inside fluid machineries. He is an expert in CFD analysis, dealing with both thermal and multiphase flows aspects. He is collaborating with Kathmandu University (KU) and Norwegian University of Science and Technology (NTNU).

Eng. Giacomo ZANETTI,
Università degli Studi di Padova
Department of Industrial Engineering
Turbomachinery & Energy Systems Research Group (TES)
Via Venezia 1, Padova, 35131, Italy
E-mail: giacomo.zanetti.4@phd.unipd.it

Eng. Giacomo Zanetti obtained his degree in Mechanical Engineering in 2021 at the University of Padova. He is a PhD student at the university of Padova financed by the company 45 Engineering. His research field includes the study of hydraulic machines with particular attention to the case of reversible pump-turbines for use in storage hydropower plants. He is author of scientific publications in International Journals with Impact Factor and in Proceedings of International Conferences.

Prof. Giovanna CAVAZZINI,
Università degli Studi di Padova
Department of Industrial Engineering
Turbomachinery & Energy Systems Research Group (TES)
Via Venezia 1, Padova, 35131, Italy
E-mail: giovanna.cavazzini@unipd.it

Prof. Giovanna Cavazzini received her degree with honour in Mechanical Engineering in 2003 from the University of Padova and her doctorate with European Label in Energetics in 2007 from the University of Padova where she works as Associate Professor since 2016. Her current research interests focus on design optimization of turbomachines with particular emphasis on the behaviour at part loads of hydraulic turbines and pump-turbines. She is author of more than 100 scientific publications, the most part of which published in International Journals with Impact Factor and in Proceedings of International Conferences.